Environmental Science & Technology

Article

Cite This: Environ. Sci. Technol. XXXX, XXX, XXX−XXX

pubs.acs.org/est

Nitrogen Speciation and Isotopic Composition of Aerosols Collected at Himalayan Forest (3326 m a.s.l.): Seasonality, Sources, and Implications

Hemraj Bhattarai,[†,#] Yan-Lin Zhang,[‡] Chandra Mouli Pavuluri,[∥] Xin Wan,[†] Guangming Wu,[†] Peilin Li,[†] Fang Cao,[‡] Wenqi Zhang,[‡] Yongjie Wang,[†] Shichang Kang,[§,∇] Kirpa Ram,[†,○] Kimitaka Kawamura,[⊥] Zhenming Ji,[◆] David Widory,[¶] and Zhiyuan Cong*[,†,∇]

[†]Key Laboratory of Tibetan Environment Changes and Land Surface Processes, Institute of Tibetan Plateau Research, Chinese Academy of Sciences, Beijing 100101, China

[‡]Yale-NUIST Center on Atmospheric Environment, Nanjing University of Information Science and Technology, 210044 Nanjing, China

[§]State Key Laboratory of Cryospheric Science, Northwest Institute of Eco-Environment and Resources, CAS, Lanzhou 730000, China

[∥]Institute of Surface-Earth System Science, Tianjin University, Tianjin 300072, China

[⊥]Chubu Institute for Advanced Studies, Chubu University, Kasugai 487-8501, Japan

[#]University of Chinese Academy of Sciences, Beijing 100049, China

[∇]CAS Center for Excellence in Tibetan Plateau Earth Sciences, Beijing 100101, China

[○]Institute of Environment and Sustainable Development, Banaras Hindu University, Varanasi 221005, India

[◆]School of Atmospheric Sciences, Guangdong Province Key Laboratory for Climate Change and Natural Disaster Studies, Sun Yat-sen University, Guangzhou 510275, China

[¶]Geotop/Université du Québec à Montréal (UQAM), 201 Ave Président Kennedy, Montréal, QC H2X 3Y7, Canada

Supporting Information

ABSTRACT: Nitrogenous aerosols are ubiquitous in the environment and thus play a vital role in the nutrient balance as well as the Earth's climate system. However, their abundance, sources, and deposition are poorly understood, particularly in the fragile and ecosensitive Himalayan and Tibetan Plateau (HTP) region. Here, we report concentrations of nitrogen species and isotopic composition ($\delta^{15}N$) in aerosol samples collected from a forest site in the HTP (i.e., Southeast Tibet). Our results revealed that both organic and inorganic nitrogen contribute almost equally with high abundance of ammonium nitrogen (NH_4^+−N) and water-insoluble organic nitrogen (WION), contributing ∼40% each to aerosol total nitrogen (TN). The concentrations and $\delta^{15}N$ exhibit a significant seasonality with ∼2 times higher in winter than in summer with no significant diurnal variations for any species. Moreover, winter aerosols mainly originated from biomass burning emissions from North India and East Pakistan and reached the HTP through a long-range atmospheric transport. The TN dry deposition and total deposition fluxes were 2.04 kg ha^{-1} yr^{-1} and 6.12 kg ha^{-1} yr^{-1} respectively. Our results demonstrate that the air contamination from South Asia reach the HTP and is most likely impacting the high altitude ecosystems in an accepted scenario of increasing emissions over South Asia.

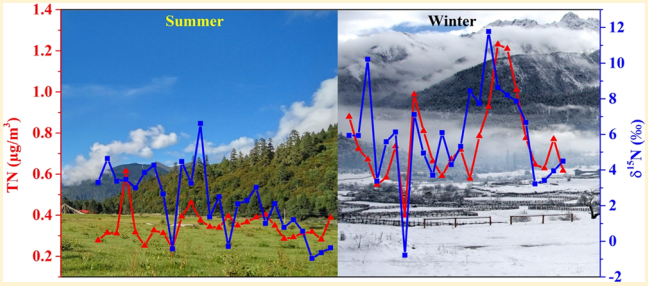

INTRODUCTION

Nitrogenous aerosols, produced by both natural and anthropogenic sources, are ubiquitous in the atmosphere. The total nitrogen (TN) mass fraction ranges from 1.2 to 17.0% in particulate matter and has noticeably increased in the last few decades.[1,2] Fossil fuel combustion and industrial emissions increase NO_x (i.e., NO and NO_2) whereas biomass burning (BB), animal husbandry, and fertilizers release aliphatic amines and ammonia (NH_3) into the atmosphere.[3,4] Furthermore, the reactions of biogenic amino acids, peptides, isoprene, volatile organic compounds (VOCs), bacteria, dust particles, and pollen with NO_3 radicals or NH_3 are the major contributors of atmospheric organic nitrogen (ON) through

Received: July 14, 2019
Revised: September 25, 2019
Accepted: September 27, 2019
Published: September 27, 2019

DOI: 10.1021/acs.est.9b03999
Environ. Sci. Technol. XXXX, XXX, XXX−XXX

gas-to-particle conversion.[5,6] All these reduced (e.g., NH_3, NH_4^+) and oxidized (e.g., NO_x, HNO_3, NO_3^-, N_2O) nitrogen species are water-soluble and can be defined as a whole as water-soluble inorganic nitrogen (WSIN). Species included in ON are both water-soluble and insoluble, making it rather difficult to quantify their abundances.

Once released into the environment, nitrogenous species can alter atmospheric chemistry and adversely affect chemical composition, human health, and climate on local, regional, and global scales.[7] Meanwhile, reactive nitrogen (i.e., N compounds that support growth directly or indirectly) is a limiting nutrient for plant growth and survival, thus affecting the nitrogen biogeochemical cycle.[8] Nevertheless, its production and deposition have triggered numerous ecological and environmental threats, ranging from eutrophication to global acidification and stratospheric ozone depletion.[9] For the year 2100, Sala et al.[10] predicted that N deposition will be the third largest driver (after land use and climate change) of global biodiversity loss. Therefore, plant diversity likely has an inverse relation with N deposition.[11]

Given their importance, nitrogenous aerosols have been studied in different geographical environments: urban cities,[12−14] coasts,[15] ocean,[16,17] forest,[6] mountains,[18] and polar regions.[19,20] Urban areas such as Delhi[21] and Beijing,[13] which are influenced by intense human activities, exhibit nitrogenous aerosol concentrations about two orders of magnitude higher than those reported over background sites such as the Antarctic[19] and the Western Pacific.[17] In recent years, considerable efforts have been made spatially and temporally to better understand the processes' controlling factors of the atmospheric budget of these nitrogenous aerosol species such as inorganic nitrogen[22] and organic nitrogen,[23,24] their sources, and physicochemical properties.

The Himalayan and Tibetan Plateau (HTP), with an average elevation of 4000 m above sea level (a.s.l.) and an area of 2.5×10^6 km^2, is one of the world's most pristine regions due to sparse population with negligible influence on its environment from local emissions. However, the recent increase in emissions and the transport of aerosols from nearby hotspots have increased the risk on its pristine nature, threatening the regional floral and faunal biodiversity.[11,25] Moreover, high concentrations have been recorded in ice cores demonstrating an increase in inorganic nitrogen deposition over the Tibetan Plateau in the last few decades.[26,27] Different models and satellite data have been used to estimate nitrogen concentrations and deposition over the HTP.[28] For example, the model estimated that Tibet receives an ∼2 kg N ha^{-1} yr^{-1} of total inorganic nitrogen deposition.[28] In contrast, ground-based studies estimated an ∼4.27 kg N ha^{-1} yr^{-1} for the total atmospheric nitrogen deposition from wet precipitation in the South-East Tibet (SET) region.[29] This wet deposition rate is already closer to the threshold (5 to 15 kg N ha^{-1} yr^{-1}) for the alpine ecosystem.[30] This indicates that the ecosystem starts to adversely react once this limit is reached, depending on the sensitivity of the ecosystem. A few studies have reported NO_3^- and NH_4^+ in aerosols from the TP for which long-range transport of anthropogenic and mineral dust was identified as a dominant source.[31] However, to our knowledge, no study has ever focused on TN atmospheric concentrations, dry deposition, and corresponding isotope compositions over HTP and thus creating a scientific gap in better understanding the fate of aerosol nitrogen over this region.

In this study, we reported measurement of the concentrations of TN, WSTN, WSIN, TON, and major ions as well as TN isotope compositions ($\delta^{15}N$) of total suspended particulate (TSP) collected during summer (August 2013) and winter (January 2014) on a day and night basis at a forest site. Source identification and characterization were further evaluated using different statistical approaches including principal component analysis (PCA), Hybrid Single-Particle Lagrangian Integrated Trajectory (HYSPLIT), and satellite data products (MODIS image, AOD, CALIPSO profile). To the best of our knowledge, this is the first study of its kind over the HTP and would serve a baseline to study different species of nitrogenous aerosols along with their possible sources in this region.

■ MATERIALS AND METHODS

Study Site Description. The South-East Tibet (SET) station of the Chinese Academy of Sciences (CAS) located at coordinates 94°44′ E, 29°46′ N, 3326 m a.s.l. (Figure S1a, Supporting Information) was selected for the TSP sample collection to study nitrogenous aerosols in the HTP. The sampling site is surrounded by a dense alpine forest (Figure S1b, Supporting Information) and is a flat grassland near the intersection of two rivers to the west and with the Himalayan mountains rising to the south. Detailed information about study site can be found in the Supporting Information.

Sample Collection. TSP aerosol samples were collected for approximately 11.5 h on pre-combusted (450 °C, 3 h) 20.3 × 25.4 cm^2 quartz fiber filters (Pallflex 2500QAT-UP, USA) using a high-volume air sampler (TH-1000 CH, Wuhan Tianhong Instrument CO., Ltd., China) at a height of 4 m above the ground (Figure S1c, Supporting Information). The air flow rate was maintained at 0.75 m^3 min^{-1} and the flow volume was automatically adjusted to standard atmospheric conditions based on the local meteorology such as temperature and pressure. The samples were collected on a day and night basis during summer 2013 (15th to 30th of August, 2013; n = 26) and winter 2014 (1st to 17th January, 2014; n = 24). The field blank samples (n = 10) were collected approximately once after every five samples at the site. All filters were carefully stored in a clean glass jar (150 mL) at a freezing temperature (<0 °C) until further analysis.[32]

Chemical Analysis. *Determination of Total Nitrogen and Its Isotopic Composition.* Concentration of bulk N and its isotopic composition ($\delta^{15}N$) were determined using 1.54 cm^2 of the filter sample. Samples were placed and sealed in a tin cup (10 × 10 mm) and analyzed using an Elemental Analyzer (Flash EA 2000) coupled to an isotope-ratio mass spectrometer (IRMS: Thermo MAT 253) at NUIST laboratory.[33] Details of the process and standards used are described in the Supporting Information.

Measurement of Inorganic Ions. The inorganic ions were extracted with 10 mL of Milli-Q ultrapure water under ultrasonication for 30 min using a 5.09 cm^2 portion of each sample filter. The extracted solution was then filtered through syringe-driven filters (ANPEL, SCAA-102, 13 mm disc, 0.22 μm) to eliminate quartz fiber debris and insoluble compounds. The filtrate was then injected into an ion chromatography (IC) instrument to quantify the major ions. More detailed information regarding instruments and processes can be found in the Supporting Information.

Measurement of Water-Soluble Total Nitrogen. Water-soluble total nitrogen (WSTN) was measured using a total

DOI: 10.1021/acs.est.9b03999
Environ. Sci. Technol. XXXX, XXX, XXX−XXX

Table 1. Seasonal and Diurnal Variations of the Concentrations of Nitrogenous Components and Water-Soluble Major Ions, and Isotope Composition of Total Nitrogen at SET, China[a]

parameters	summer (26)			winter (24)			overall (50)av. ± SD (min−max)
	day (13)	night (13)	av (26)	day (12)	night (12)	av (24)	
nitrogenous species concentrations (μg m^{-3})							
TN	0.33 ± 0.06	0.36 ± 0.08	0.35 ± 0.07	0.76 ± 0.21	0.76 ± 0.19	0.76 ± 0.20	0.54 ± 0.25 (0.24−1.23)
WSTN	0.21 ± 0.10	0.17 ± 0.06	0.19 ± 0.09	0.46 ± 0.22	0.49 ± 0.25	0.47 ± 0.24	0.33 ± 0.23 (0.05−0.99)
WSIN	0.18 ± 0.10	0.16 ± 0.10	0.16 ± 0.10	0.38 ± 0.19	0.42 ± 0.17	0.40 ± 0.18	0.27 ± 0.19 (0.01−0.75)
TON	0.16 ± 0.08	0.21 ± 0.11	0.19 ± 0.10	0.38 ± 0.09	0.33 ± 0.08	0.36 ± 0.09	0.27 ± 0.13 (BDL−0.52)
NO_2^- −N	0.0 ± 0.010	0.01 ± 0.02	0.01 ± 0.02	0.03 ± 0.03	0.02 ± 0.02	0.02 ± 0.02	0.02 ± 0.02 (BDL−0.08)
NO_3^- −N	0.03 ± 0.01	0.02 ± 0.01	0.03 ± 0.01	0.07 ± 0.02	0.06 ± 0.02	0.06 ± 0.02	0.04 ± 0.02 (0.01−0.10)
NH_4^+ −N	0.14 ± 0.10	0.11 ± 0.09	0.13 ± 0.09	0.28 ± 0.16	0.34 ± 0.16	0.31 ± 0.16	0.22 ± 0.16 (BDL−0.66)
WSON	0.04 ± 0.03	0.04 ± 0.04	0.04 ± 0.04	0.09 ± 0.07	0.09 ± 0.10	0.09 ± 0.09	0.06 ± 0.07 (BDL−0.34)
WION	0.12 ± 0.08	0.17 ± 0.11	0.15 ± 0.10	0.29 ± 0.10	0.24 ± 0.10	0.27 ± 0.10	0.21 ± 0.12 (BDL−0.45)
isotope composition (‰)							
δ^{15}N	1.68 ± 1.59	2.72 ± 1.96	2.20 ± 1.86	5.73 ± 2.74	6.13 ± 2.41	5.93 ± 2.59	3.99 ± 2.91 (−0.96 to 11.78)
major ions concentrations (μg m^{-3})							
Cl^-	0.15 ± 0.06	0.16 ± 0.11	0.15 ± 0.09	0.15 ± 0.06	0.19 ± 0.10	0.17 ± 0.08	0.16 ± 0.09 (0.05−0.39)
NO_2^-	0.09 ± 0.06	0.12 ± 0.10	0.10 ± 0.09	0.19 ± 0.10	0.16 ± 0.07	0.18 ± 0.09	0.14 ± 0.10 (0.03−0.43)
NO_3^-	0.12 ± 0.04	0.11 ± 0.05	0.11 ± 0.04	0.29 ± 0.09	0.25 ± 0.07	0.27 ± 0.09	0.19 ± 0.10 (0.05−0.42)
SO_4^{2-}	0.65 ± 0.39	0.53 ± 0.27	0.59 ± 0.34	1.38 ± 0.58	1.47 ± 0.55	1.43 ± 0.57	0.99 ± 0.62 (0.06−2.51)
Na^+	0.06 ± 0.03	0.06 ± 0.03	0.06 ± 0.03	0.06 ± 0.01	0.05 ± 0.01	0.05 ± 0.01	0.06 ± 0.02 (0.03−0.16)
NH_4^+	0.19 ± 0.13	0.16 ± 0.11	0.18 ± 0.12	0.38 ± 0.21	0.46 ± 0.20	0.42 ± 0.21	0.29 ± 0.21 (BDL−0.87)
K^+	0.06 ± 0.01	0.08 ± 0.01	0.07 ± 0.01	0.13 ± 0.04	0.12 ± 0.04	0.12 ± 0.04	0.09 ± 0.04 (0.04−0.20)
Mg^{2+}	0.01 ± 0.01	0.01 ± 0.00	0.01 ± 0.01	0.02 ± 0.01	0.01 ± 0.01	0.02 ± 0.01	0.01 ± 0.01 (BDL−0.06)
Ca^{2+}	0.16 ± 0.10	0.08 ± 0.07	0.12 ± 0.09	0.69 ± 0.40	0.25 ± 0.19	0.47 ± 0.38	0.29 ± 0.32 (0.01−1.79)

[a]BDL: below detection limits (4 ppb for nitrogenous species and 1 ppb for major ions).

organic carbon (TOC)/TN analyzer (Shimadzu TOC-L) with a 4 μg/L detection limit. Three 18 mm-diameter filter cuts (total surface area of ca. 7.63 cm^2) were extracted in 15 mL of ultrapure Milli-Q water (18.2 MΩ.cm) under an ultrasonic bath for 30 min at room temperature and pressure. The extracted solution was passed through 13 mm disc filters with a 0.22 μm pore size, and the solutes were analyzed using the TOC/TN analyzer.

Estimation of Organic Nitrogen. Total organic nitrogen (TON), water-soluble ON (WSON), and water-insoluble ON (WION) were calculated using the following equations.[16]

$$\mathrm{TON} = \mathrm{TN} - \mathrm{WSIN} \tag{1a}$$

$$\mathrm{WSON} = \mathrm{WSTN} - \mathrm{WSIN} \tag{1b}$$

$$\mathrm{WION} = \mathrm{TN} - \mathrm{WSTN} \tag{1c}$$

TN and WSTN were directly obtained from the instruments described above. WSIN is the sum of the IN species (NH_4^+−N + NO_3^-−N + NO_2^-−N). Based on the error propagation of each parameter, the measured uncertainty for ON was estimated to be ∼6%.

Backward Air Mass Trajectories and Active Fire Spots. Five-day backward air mass trajectories arriving at a 500 m height above ground level (a.g.l.) were computed using the HYSPLIT model to identify the most likely pathway and potential source regions of the air masses observed at the SET station.[34] Meteorological data were taken from the Global Data Assimilation System (GDAS, 1 degree, 2006−present), taking into account that the accuracy of the calculated trajectories is mainly governed by their spatial and temporal variations.[35,36] The Fire Information and Resource Management System (FIRMS) developed by NASA (https://earthdata.nasa.gov/earth-observation-data/near-real-time/firms/) was used to identify the active fire spots during the sampling period.

Dry Deposition Flux. Dry deposition fluxes (F) were calculated by multiplying the dry deposition velocity (V_d) by the concentration of nitrogenous species in the aerosol samples (C):[37]

$$F = V_d \times C \tag{2}$$

In this study, V_d of nitrogenous aerosols was obtained from a previous study of TSP samples.[38] The deposition velocities used in this study for TN, ON, and NO_3^- was 1.2 cm s^{-1} and for NH_4^+ was 0.6 cm s^{-1}. These V_d for particulate NO_3^- and NH_4^+ were much closer to the one used by Fu et al.[39] for forest ecosystems in China. Similar deposition velocity for NO_3^- was also applied by Chen and Huang[40] to calculate the deposition flux over the South China Sea. Nonetheless, it should be noted that V_d is influenced by gravitational settling, impaction and diffusion of particles, particulate size, geographical locations, and meteorological parameters (e.g., relative humidity, atmospheric pressure, and wind speed), which could vary with the season. The difference in V_d may shift the calculated flux by a factor of 2−3.[37]

RESULTS AND DISCUSSION

Concentration and Speciation of Nitrogen Species in Aerosols. Concentrations of TN, nitrogen species, and major ions are presented in Table 1. TN, WSTN, WSIN, and TON concentrations in aerosols from SET station ranged from 0.24 to 1.23 μg m^{-3} (0.54 ± 0.25 μg m^{-3}), 0.05 to 0.99 μg m^{-3} (0.33 ± 0.23 μg m^{-3}), 0.01 to 0.75 μg m^{-3} (0.27 ± 0.19 μg m^{-3}), and below detection limit (BDL) to 0.52 μg m^{-3} (0.27 ± 0.13 μg m^{-3}), respectively. The WSIN species such as NH_4^+−N, NO_3^-−N, and NO_2^-−N have average concentrations of 0.22 ± 0.16, 0.04 ± 0.02, and 0.02 ± 0.02 μg m^{-3}, respectively.

The average concentration of TN at the SET station was slightly lower than those reported in Okinawa Island of Japan

DOI: 10.1021/acs.est.9b03999
Environ. Sci. Technol. XXXX, XXX, XXX−XXX

(0.72 μg m^{-3}),[41] Yongxing Island of South China Sea (0.77 μg m^{-3})[42] as well as in $PM_{2.5}$ (0.7 μg m^{-3}) and PM_{10} (0.8 μg m^{-3}) at a rural site in Tanzania.[43] However, the observed TN value of 0.54 ± 0.25 μg m^{-3} is about 20 to 50 times lower than that reported for Asian urban sites such as Delhi,[21] Kolkata,[14] and Beijing.[13] In contrast, the TN concentrations measured at the SET station were slightly higher than that reported in marine aerosols from the central North Pacific (0.37 μg m^{-3}),[44] and even higher than that in Antarctic (0.056 μg m^{-3})[19] (Table S1, Supporting Information). The lower TN concentration at the SET station supports the idea that the Tibetan Plateau can be considered as a relatively clean site and thus represents a regional background site.

Aerosol nitrogen composition shows that abundances of ON (49.46%) are almost equal to that of IN (50.54%). The ON and IN are mainly composed of WION and NH_4^+−N respectively with contributions of ∼37.7% and ∼39.8% of the TN, respectively (Figure 1). The other TN compounds such as water-soluble organic nitrogen (WSON), NO_3^--N and NO_2^-−N contribute only 11.7%, 7.8%, and 2.8% of TN, respectively. Surprisingly, the observed ON fraction over TP (49.4%) is significantly higher compared to those over a forest site in the Southeast US (33%)[45] and a rural site in central Europe (27%).[2] Moreover, it is much higher than that in urban Beijing (7−10%)[24] but lower than that in marine aerosols (67%).[16] The abundance of NH_4^+ is larger than that of NO_3^- and is similar to those over a mountain site in India (Nainital).[18] However, this is in contrast to those over mega cities such as Delhi[46] or Beijing[13] where NO_3^- abundance is larger than that of NH_4^+. These are due to the fact that emission sources of NH_4^+ and NO_3^- are very different over urban and rural environments. The higher NO_3^- concentrations observed in urban sites mostly result from the influence of road traffic, industries, and residential sources, whereas the higher concentration of NH_4^+ in rural sites are mostly linked to biomass burning, agricultural activities, and human and animal excreta.[3,13]

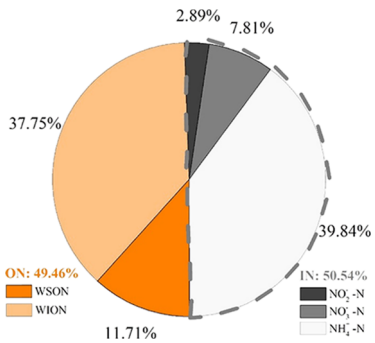

Figure 1. Total nitrogen (TN) composition in the aerosol samples from the SET. The area enclosed within the dotted line indicates the IN.

Seasonal and Diurnal Patterns for TN, WSTN, WSIN, and TON. Nitrogen species showed significant seasonal variation with higher average concentrations in winter compared to summer (Figure 2 and Table 1). Seasonally average concentrations of TN, WSTN, WSIN, and TON in summer (and winter, values in brackets) were 0.35 ± 0.07 μg m^{-3} (0.76 ± 0.20 μg m^{-3}), 0.19 ± 0.09 μg m^{-3} (0.47 ± 0.24 μg m^{-3}), 0.16 ± 0.10 μg m^{-3} (0.40 ± 0.18 μg m^{-3}) and 0.19 ± 0.10 μg m^{-3} (0.36 ± 0.09 μg m^{-3}), respectively. The analysis reflects that concentrations of all the species in winter were approximately twice higher compared to those of summer. In addition, the absence of significant day/night variations in both seasons ($P > 0.05$) indicates that local emissions, boundary layer dynamics, and meteorological parameters, such as temperature or solar radiation, did not control the nitrogenous

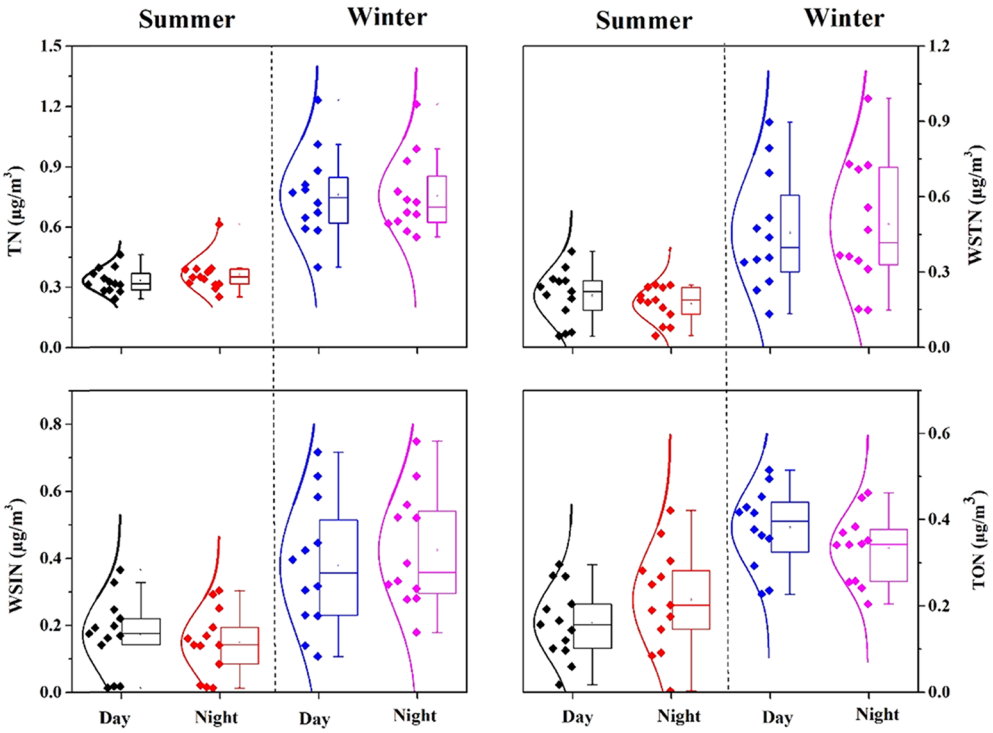

Figure 2. Box and whisker plots of the seasonal and diurnal variations of TN, WSTN, WSIN, and TON in the aerosol samples at the SET station.

DOI: 10.1021/acs.est.9b03999
Environ. Sci. Technol. XXXX, XXX, XXX−XXX

aerosol budget at SET. The possible reasons are discussed in the following sections.

Total Nitrogen Isotopic Compositions. Identification of sources, especially for aerosol nitrogen species, in the atmosphere is challenging due to their various emission sources (e.g., biomass burning, fossil fuel combustion, agricultural practices, and animal husbandry) and potential secondary transformation through post emission processes. However, isotopic composition of nitrogen (δ^{15}N) has demonstrated the additional importance in identifying sources and characterizing processes controlling the budget of atmospheric nitrogen.[18,41,47,48] Previous studies have demonstrated that δ^{15}N vary among emission sources, although some overlap exists.[49] While biomass burning results in δ^{15}N enrichment (2.0 to 25.7‰),[43,50−53] fossil fuel combustion yields δ^{15}N depletion (fuel oil: −19.4 to 2.9‰, coal: −5.3‰, unleaded gasoline: 4.6‰ and diesel: 3.9 to 5.4‰).[12] Most of the δ^{15}N ranges from −0.9 to 4.6‰ in summer, which suggests inputs from mixed sources, whereas those of 3.3 to 11.7‰ in winter, suggesting the dominant contribution from biomass burning. Moreover, the stable isotope approach has shown good ability to constrain not only different emission sources but also potential secondary formation in aerosols by specific δ^{15}N isotopic signatures.[12,54]

δ^{15}N of total nitrogen in the aerosol samples collected from the SET station ranged from −0.9 to 11.7‰ (3.9 ± 2.9‰) (Table 1). Similar to the abundance, δ^{15}N also displayed significant seasonal variations, with a higher average value in winter (5.9 ± 2.5‰) than in summer (2.2 ± 1.8‰), although the diurnal variation of δ^{15}N was not significant ($P > 0.05$) (Figure 3). The δ^{15}N observed in this study is slightly lower

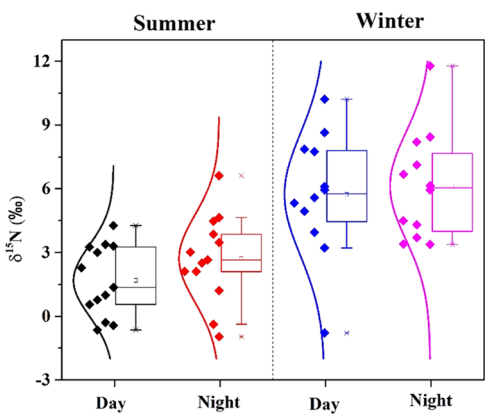

Figure 3. Seasonal and diurnal variations of the δ^{15}N measured in the aerosol samples collected at the SET station.

than those from cities closer to the Himalayas such as Kolkata, India[14] and Kathmandu, Nepal.[55] In contrast, δ^{15}N values are much lower than those compared to other urban sites such as Chennai,[48] Mumbai,[56] and Nainital[18] in India, Beijing in China,[13] Dai Ang Khang in Thiland,[57] and Morogoro in Tanzania[43] (Figure S2, Supporting Information). However, the seasonal pattern at the SET station (i.e., higher δ^{15}N in winter) located on the northern slope of the Himalayas is similar to that reported on the southern side of Himalayas such as Nainital.[18]

Although δ^{15}N indicated the presence of different sources of nitrogen in summer and winter seasons we found a positive linear correlation between δ^{15}N and TN ($R = 0.74$, $P < 0.01$; Figure 4). This may imply that summertime TN concentrations and δ^{15}N values ultimately increased with biomass

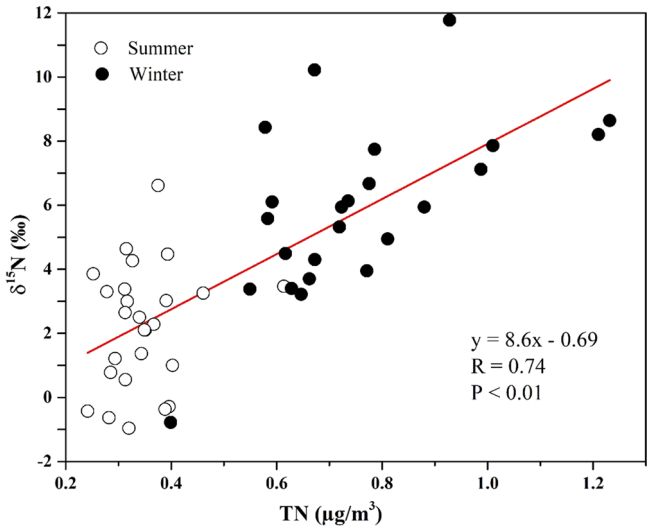

Figure 4. Linear correlation between TN and its corresponding isotope composition (δ^{15}N) during summer (white circles) and winter (black circles).

burning emissions in winter. δ^{15}N variations may also be affected by the isotopic fractionation due to the enhanced formation of secondary nitrogen in the aerosols. Furthermore, the chemical aging of ammonium and sulfate could enrich the δ^{15}N value. In a recent study over central Europe, the δ^{15}N was found to be enriched in the BB aerosols due to ammonium and sulfate aging.[2] Moreover, an overlap of δ^{15}N may occur in presence of multiple sources and/or of different formation processes.[2] Overall, we observed significant positive correlation between δ^{15}N and IN species such as NO_3^-−N ($R = 0.80$, $P < 0.01$) and NH_4^+−N ($R = 0.73$, $P < 0.01$) (Figure S3, Supporting Information). However, the correlation between δ^{15}N and TON was poor ($R = 0.32$, $P < 0.05$). The Pearson's correlation also indicates that there is a significant correlation between δ^{15}N and the IN for both seasons (Table S2). These result imply that δ^{15}N of TN is largely influenced by NO_3^-−N and NH_4^+−N species. Therefore, the emission sources and formation of NO_3^-−N and NH_4^+−N could have a major control on the variations of TN isotope compositions.

Nitrogen Sources Identification. We also analyzed several water-soluble major ions in order to identify the potential sources of nitrogenous aerosols in our study area. Results showed that SO_4^{2-} yields a moderate correlation with NO_3^-−N ($R = 0.74$, $P < 0.01$) and a strong correlation with NH_4^+−N ($R = 0.97$, $P < 0.01$) (Figure 5). Similarly, K^+ also correlated with NO_3^-−N ($R = 0.81$, $P < 0.01$) and NH_4^+−N ($R = 0.82$, $P < 0.01$). The positive correlations of inorganic nitrogen species with SO_4^{2-} and K^+ confirm our previous conclusions, that is, biomass burning dominantly contributes to the nitrogen budget in aerosols. These K^+ and SO_4^{2-} are simultaneously originated by biomass burning activities.[58−60] The earlier observations also reported that NH_4^+, NO_3^-, K^+, and SO_4^{2-} are jointly originating from biomass burning in the southeastern Tibetan Plateau[61] and Himalayas.[62] Furthermore, based on the transmission electron microscopy (TEM) analysis, the existence of K_2SO_4 and KNO_3 was found in aged biomass burning aerosols.[63] All of these considerations

DOI: 10.1021/acs.est.9b03999
Environ. Sci. Technol. XXXX, XXX, XXX−XXX

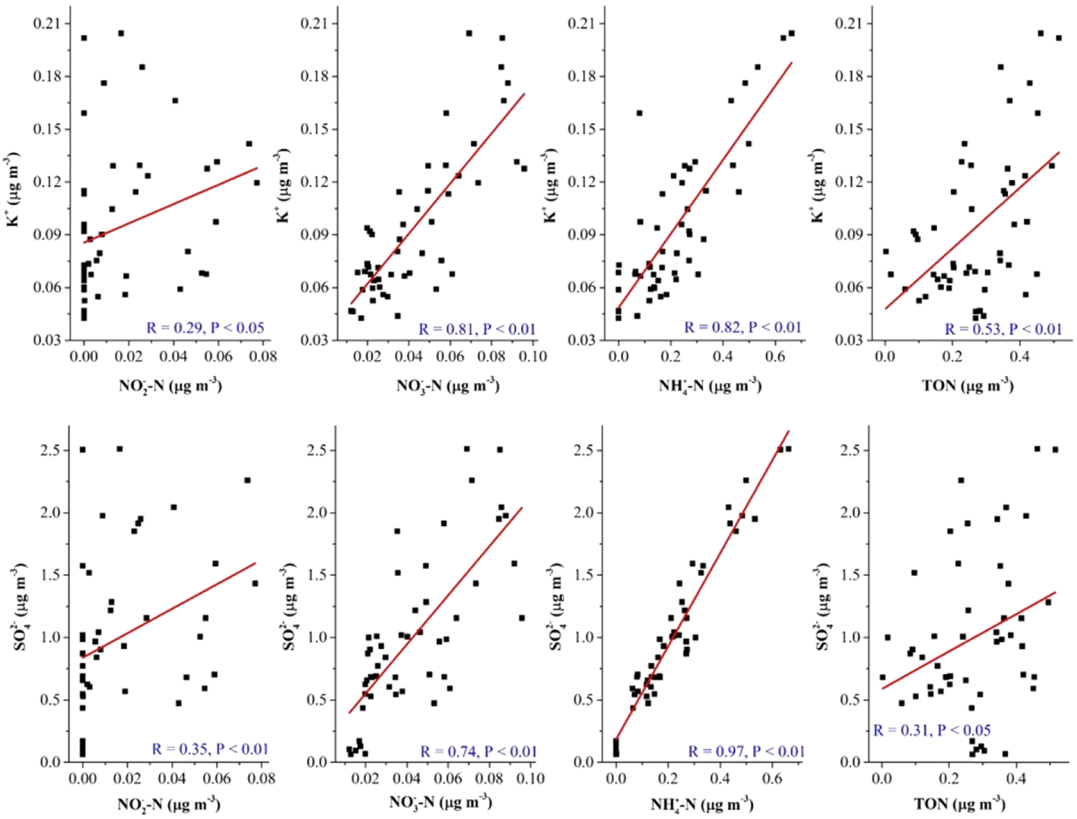

Figure 5. Linear correlation between K^+, SO_4^{2-}, and different nitrogen species: NO_2^-−N, NO_3^-−N, NH_4^+−N, and TON.

conclude that K^+ and SO_4^{2-} co-exist in biomass burning particles as a major source of nitrogenous aerosols.

The corresponding seasonal Pearson's correlation coefficients, calculated for the different nitrogenous species and major ions, are presented in Table S2 of the Supporting Information. The results further highlight that the correlation between TN and K^+ (used as a BB proxy) is stronger in winter ($R = 0.86$, $P < 0.01$) than in summer ($R = 0.62$, $P < 0.01$). This again suggests the extensive influence of BB, especially in winter, although it could be argued that K^+ can also come from crustal sources. However, there is no significant ($P > 0.05$) correlation between K^+ and crustal elements such as Ca^{2+}, supporting that biomass burning is the most likely source of nitrogenous aerosols. Moreover, significant ($P < 0.01$) correlations among NH_4^+, NO_3^-, and K^+ in winter again demonstrate a BB origin. Once released into the environment, gaseous NH_3 can react with nitric and sulfuric acids to form ammonium nitrate and ammonium sulfate/bisulfate, which ultimately contribute to atmospheric particles as NH_4^+.[7] A strong linear correlation was also observed between SO_4^{2-} and NH_4^+ during both summer ($R = 0.94$, $P < 0.01$) and winter ($R = 0.97$, $P < 0.01$) (Table S2, Supporting Information), indicating a common source of contamination, mostly related to biomass burning emissions.

On the other hand, ON showed no significant correlation with neither Na^+ (sea spray), K^+ (BB), nor Ca^{2+} (crustal) (Table S2, Supporting Information). This result indicates that ON at the SET station is not generated by primary sources but is rather derived from secondary processes. Common ON compounds, such as hydroxyalkyl nitrates, are generally produced by reaction of gas phase NO_x with VOCs.[5,42] WION, which is dominant in ON, is mostly produced via the reaction of gaseous hydrocarbons with NH_3.[1,5] Moreover, some of the other pathways leading to the formation of ON are mostly related to agricultural activities, biological particles, or secondary processes.[23]

In addition, different chemical species were subjected to a principal component analysis (PCA) by Kaiser Normalization under the direct varimax rotation statistical technique using the SPSS statistics 16.0 software. In summer, Na^+ and Cl^- were closely associated with oxidized IN (NO_2^- and NO_3^-), whereas in winter they were not correlated (Figure S4, Supporting Information). This suggests a possibility of marine contribution during summer at the SET station, being in agreement with the previous findings.[29] Similarly, NO_3^- in winter and NH_4^+ for both seasons were closely linked to K^+ and SO_4^{2-}, supporting a contribution from BB emissions. However, crustal elements such as Ca^{2+} and Mg^{2+} do not correlate with other ionic species in winter and, to lesser extent, in summer, again supporting the conclusion that they play no significant role in the aerosol budget over the study area.

Possible Transport Pathway and Air-Mass Trajectories and Satellite Observations. The discussions above identified biomass burning as the major source of nitrogenous aerosols over the study area. In order to investigate the potential source regions, we computed five-day air mass back-trajectories using the HYSPLIT model, coupled with the active fire map generated by the NASA moderate-resolution imaging spectroradiometer (MODIS) over the periods of the summer and winter campaign (Figure 6). Results showed that air mass trajectories reaching at the SET station can be divided into two distinct groups: (a) winds blowing from the Bay of Bengal during summer or (b) winds originating from the Indo-

DOI: 10.1021/acs.est.9b03999
Environ. Sci. Technol. XXXX, XXX, XXX−XXX

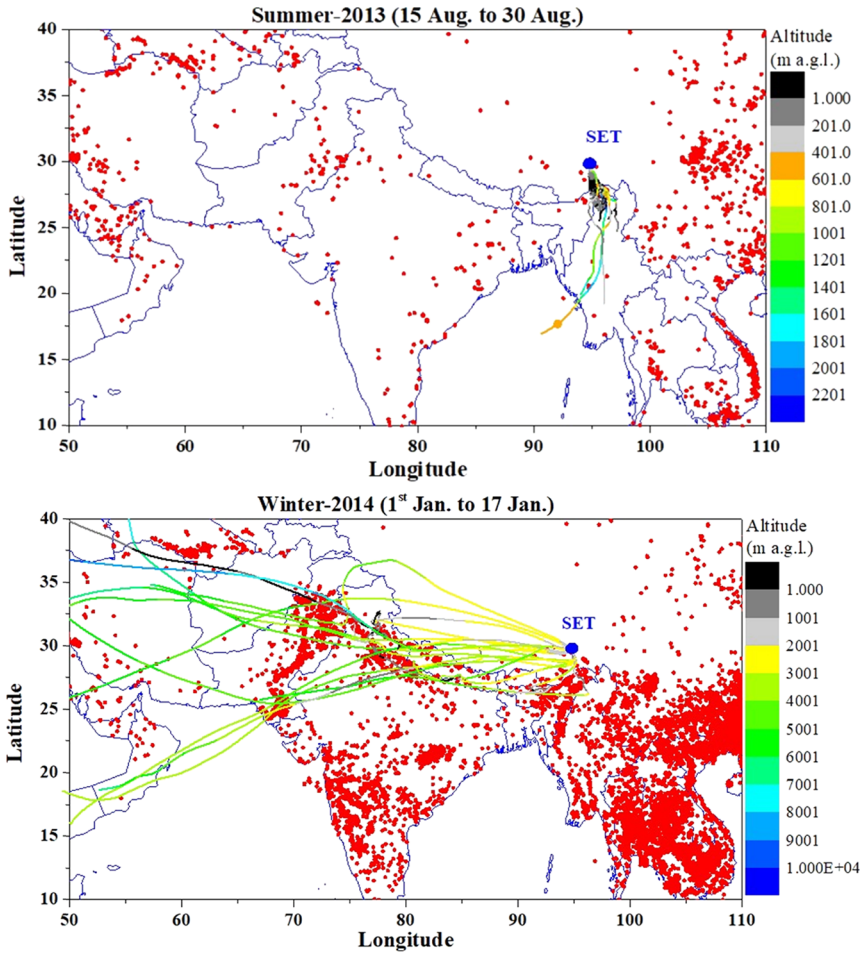

Figure 6. Five-day air mass back trajectories (500 m a.g.l.) in summer (top) and winter (bottom) over Lulang, SET station, China. The red dots represent the active fire spots during the sampling period obtained from NASA (https://earthdata.nasa.gov/earth-observation-data/near-real-time/firms/active-fire-data).

Gangetic Plain (IGP) region (North-West India and Eastern Pakistan) during winter. In addition, dense fire spots were detected in the IGP during winter (Figure 6), with surrounding areas showing intensive haze and air pollution plumes (3 Jan 2014, Figure S6b of the Supporting Information), compared to summer (19 August 2013, Figure S6a, Supporting Information). Similar to our findings, previous studies also reported intensive biomass burning in the IGP region during wintertime.[64] Aerosol Optical Depth (AOD) at 0.55 μm also showed higher aerosol concentrations in winter than summer in the IGP region (Figure S6c,d, Supporting Information). The thick haze and AOD observed in the IGP region largely result from the biomass burning emissions and high relative humidity, which lower the boundary layer height and are conducive for haze formation.[65,66] Thus, the coupled data of the air mass back-trajectories and MODIS fire spots demonstrate that seasonal variation of the concentrations of TN and its nitrogen species were controlled by long-range transport and biomass burning emissions from the IGP region. In addition, the Cloud-Aerosol Lidar with Orthogonal Polarization (CALIOP) provides aerosol vertical profiles: during summer, the contamination plume can reach an altitude of 15 km (August 19, Figure S5 of the Supporting Information), whereas in winter it can reach an altitude of 4−5 km (January 3, Figure S5, Supporting Information), which is enough in both cases to bypass/cross the Himalayas and reach the TP. Cong, et al.[67] reported the contribution of valley winds and glacial winds in transporting pollutants from the IGP to the Himalayan and Tibetan Plateau.

Estimation of Dry Deposition Flux and Environmental Implications. Humans have altered the global nitrogen cycle, in particular by the intense release of reactive nitrogen species into the environment.[68] The deposition (either dry or wet) of these nitrogen species over terrestrial and aquatic ecosystems has implications for both biological diversity and human and ecosystem health.[69] Therefore, the estimation of dry deposition flux is essential in predicting the impact of aerosols on the Himalayan ecosystem. However, the measurement is not easy, especially in alpine ecosystems. Here, we have estimated dry deposition flux from the measured concentration of NO_3^-, NH_4^+, ON, and TN in SET (Table S3, Supporting Information). The average annual dry deposition fluxes were estimated for NO_3^-, NH_4^+, ON, and TN as 0.72, 0.55, 1.02, and 2.04 kg ha^{-1} yr^{-1} respectively. Atmospheric nitrogen depositions over the SET are similar to those over the Rocky mountains in Colorado[70] but much lower than those reported for urban environments.[71] The Rocky mountain region in Colorado, with a similar altitude and environment, showed dry deposition of approximately 25 to 47% of TN atmospheric deposition (Burns[70] and reference therein). Therefore, TN wet deposition is assumed to be double of dry deposition, which is in accordance with the earlier result

DOI: 10.1021/acs.est.9b03999
Environ. Sci. Technol. XXXX, XXX, XXX−XXX

over TP[29] and Rocky mountain.[70] The estimated wet deposition is ~4.08 kg ha^{-1} yr^{-1} at our study area. The above estimations omitted the fog and cloud deposition, which could be significant at alpine forest ecosystems. Thus, the total atmospheric nitrogen deposition (dry plus wet) at the SET should be higher than 6.12 kg ha^{-1} yr^{-1}. This already exceeded the lower limit (5 kg ha^{-1} yr^{-1}) of critical load reported for alpine ecosystem (5−15 kg ha^{-1} yr^{-1}).[30] Moreover, the estimated total nitrogen deposition is around two times the global terrestrial average N deposition (3.5 kg ha^{-1} yr^{-1}).[11] Studies have identified N deposition on terrestrial and aquatic ecosystems as a serious threat to the world floristic diversity.[11] Lichens and bryophytes, which are important species in alpine forest of the SET, are sensitive to elevated N inputs.[29,30] NO_3^- and NH_4^+, the major nitrogen components in aerosols, are readily available to plants and microorganisms, acting as limiting nutrients for the existing systems. These species could change the aquatic and terrestrial life, affecting pristine ecosystems.

■ ASSOCIATED CONTENT

Supporting Information

The Supporting Information is available free of charge on the ACS Publications website at DOI: 10.1021/acs.est.9b03999.

TN concentration comparison, Pearson correlation matrix, dry deposition fluxes, sampling site location, δ^{15}N comparison, δ^{15}N correlation with TN species, principal component analysis, and results from CALIPSO and MODIS (PDF)

■ AUTHOR INFORMATION

Corresponding Author

*E-mail: zhiyuancong@itpcas.ac.cn.

ORCID

Yan-Lin Zhang: 0000-0002-8722-8635
Chandra Mouli Pavuluri: 0000-0002-2955-474X
Guangming Wu: 0000-0002-7043-8169
Kimitaka Kawamura: 0000-0003-1190-3726
Zhiyuan Cong: 0000-0002-7545-5611

Notes

The authors declare no competing financial interest.

■ ACKNOWLEDGMENTS

This study was supported by the Strategic Priority Research Program of the Chinese Academy of Sciences, the Pan-Third Pole Environment Study for a Green Silk Road (Pan-TPE) (XDA20040501), and the National Natural Science Foundation of China (41877315, 41807389, and 41761144056). We acknowledge Prof. Xiande Liu for his constructive suggestions. We also thank Dr. Shaopeng Gao for helping during the lab work and the staff at SET station for help in field sampling.

■ REFERENCES

(1) Pavuluri, C. M.; Kawamura, K.; Fu, P. Q. Atmospheric chemistry of nitrogenous aerosols in northeastern Asia: biological sources and secondary formation. *Atmos. Chem. Phys.* **2015**, *15*, 9883−9896.

(2) Vodička, P.; Kawamura, K.; Schwarz, J.; Kunwar, B.; Ždímal, V. Seasonal study of stable carbon and nitrogen isotopic composition in fine aerosols at a Central European rural background station. *Atmos. Chem. Phys.* **2019**, *19*, 3463−3479.

(3) Van Damme, M.; Clarisse, L.; Whitburn, S.; Hadji-Lazaro, J.; Hurtmans, D.; Clerbaux, C.; Coheur, P.-F. Industrial and agricultural ammonia point sources exposed. *Nature* **2018**, *564*, 99−103.

(4) Bray, C. D.; Battye, W.; Aneja, V. P.; Tong, D. Q.; Lee, P.; Tang, Y. Ammonia emissions from biomass burning in the continental United States. *Atmos. Environ.* **2018**, *187*, 50−61.

(5) Jickells, T.; Baker, A. R.; Cape, J. N.; Cornell, S. E.; Nemitz, E. The cycling of organic nitrogen through the atmosphere. *Philos. Trans. R. Soc., B* **2013**, *368*, 20130115.

(6) Miyazaki, Y.; Fu, P.; Ono, K.; Tachibana, E.; Kawamura, K. Seasonal cycles of water-soluble organic nitrogen aerosols in a deciduous broadleaf forest in northern Japan. *J. Geophys. Res.: Atmos.* **2014**, *119*, 1440−1454.

(7) Seinfeld, J. H.; Pandis, S. N. *Atmospheric chemistry and physics: from air pollution to climate change*; John Wiley & Sons: 2016.

(8) Elser, J. J.; Bracken, M. E. S.; Cleland, E. E.; Gruner, D. S.; Harpole, W. S.; Hillebrand, H.; Ngai, J. T.; Seabloom, E. W.; Shurin, J. B.; Smith, J. E. Global analysis of nitrogen and phosphorus limitation of primary producers in freshwater, marine and terrestrial ecosystems. *Ecol. Lett.* **2007**, *10*, 1135−1142.

(9) Gruber, N.; Galloway, J. N. An Earth-system perspective of the global nitrogen cycle. *Nature* **2008**, *451*, 293−296.

(10) Sala, O. E.; Chapin, F. S., III; Armesto, J. J.; Berlow, E.; Bloomfield, J.; Dirzo, R.; Huber-Sanwald, E.; Huenneke, L. F.; Jackson, R. B.; Kinzig, A.; Leemans, R.; Lodge, D. M.; Mooney, H. A.; Oesterheld, M.; Poff, N. L.; Skykes, M. T.; Walker, B. H.; Walker, M.; Wall, D. H. Global Biodiversity Scenarios for the Year 2100. *Science* **2000**, *287*, 1770−1774.

(11) Phoenix, G. K.; Hicks, W. K.; Cinderby, S.; Kuylenstierna, J. C. I.; Stock, W. D.; Dentener, F. J.; Giller, K. E.; Austin, A. T.; Lefroy, R. D. B.; Gimeno, B. S.; Ashmore, M. R.; Ineson, P. Atmospheric nitrogen deposition in world biodiversity hotspots: the need for a greater global perspective in assessing N deposition impacts. *GCB* **2006**, *12*, 470−476.

(12) Widory, D. Nitrogen isotopes: tracers of origin and processes affecting PM 10 in the atmosphere of Paris. *Atmos. Environ.* **2007**, *41*, 2382−2390.

(13) He, N.; Kawamura, K.; Kanaya, Y.; Wang, Z. Diurnal variations of carbonaceous components, major ions, and stable carbon and nitrogen isotope ratios in suburban aerosols from northern vicinity of Beijing. *Atmos. Environ.* **2015**, *123*, 18−24.

(14) Sharma, S. K.; Mandal, T. K.; Shenoy, D. M.; Bardhan, P.; Srivastava, M. K.; Chatterjee, A.; Saxena, M.; Saraswati; Singh, B.; Ghosh, S. K. Variation of Stable Carbon and Nitrogen Isotopic Composition of PM10 at Urban Sites of Indo Gangetic Plain (IGP) of India. *Bull. Environ. Contam. Toxicol.* **2015**, *95*, 661−669.

(15) Chen, H. Y.; Chen, L. D.; Chiang, Z. Y.; Hung, C. C.; Lin, F. J.; Chou, W. C.; Gong, G. C.; Wen, L. S. Size fractionation and molecular composition of water-soluble inorganic and organic nitrogen in aerosols of a coastal environment. *J. Geophys. Res.: Atmos.* **2010**, *115*, D22307.

(16) Miyazaki, Y.; Kawamura, K.; Jung, J.; Furutani, H.; Uematsu, M. Latitudinal distributions of organic nitrogen and organic carbon in marine aerosols over the western North Pacific. *Atmos. Chem. Phys.* **2011**, *11*, 3037−3049.

(17) Kawamura, K. Total Carbon and Nitrogen Contents and Molecular Composition of Water Soluble Organic Matter in the Marine Aerosols from Western North to Tropical Central Pacific. In *Dynamics and Characterization of Marine Organic Matter*,: Springer: 2000; pp 465−484.

(18) Hegde, P.; Kawamura, K.; Joshi, H.; Naja, M. Organic and inorganic components of aerosols over the central Himalayas: winter and summer variations in stable carbon and nitrogen isotopic composition. *Environ. Sci. Pollut. Res.* **2016**, *23*, 6102−6118.

(19) Kawamura, K.; Seméré, R.; Imai, Y.; Fujii, Y.; Hayashi, M. Water soluble dicarboxylic acids and related compounds in Antarctic aerosols. *J. Geophys. Res.: Atmos.* **1996**, *101*, 18721−18728.

(20) Dall'Osto, M.; Ovadnevaite, J.; Paglione, M.; Beddows, D. C. S.; Ceburnis, D.; Cree, C.; Cortés, P.; Zamanillo, M.; Nunes, S. O.;

DOI: 10.1021/acs.est.9b03999
Environ. Sci. Technol. XXXX, XXX, XXX−XXX

Pérez, G. L.; Ortega-Retuerta, E.; Emelianov, M.; Vaqué, D.; Marrasé, C.; Estrada, M.; Sala, M. M.; Vidal, M.; Fitzsimons, M. F.; Beale, R.; Airs, R.; Rinaldi, M.; Decesari, S.; Cristina Facchini, M.; Harrison, R. M.; O'Dowd, C.; Simó, R. Antarctic sea ice region as a source of biogenic organic nitrogen in aerosols. *Sci. Rep.* **2017**, *7*, 6047.

(21) Sen, A.; Karapurkar, S. G.; Saxena, M.; Shenoy, D. M.; Chaterjee, A.; Choudhuri, A. K.; Das, T.; Khan, A. H.; Kuniyal, J. C.; Pal, S.; Singh, D. P.; Sharma, S. K.; Kotnala, R. K.; Mandal, T. K. Stable carbon and nitrogen isotopic composition of PM10 over Indo-Gangetic Plains (IGP), adjoining regions and Indo-Himalayan Range (IHR) during a winter 2014 campaign. *Environ. Sci. Pollut. Res.* **2018**, *25*, 26279−26296.

(22) Liu, Y. W.; Xu-Ri; Wang, Y. S.; Pan, Y. P.; Piao, S. L. Wet deposition of atmospheric inorganic nitrogen at five remote sites in the Tibetan Plateau. *Atmos. Chem. Phys.* **2015**, *15*, 11683−11700.

(23) Nehir, M.; Koçak, M. Atmospheric Water-Soluble Organic Nitrogen (WSON) in the Eastern Mediterranean: Origin and Ramifications Regarding Marine Productivity. *Atmos. Chem. Phys.* **2018**, *18*, 3603−3618.

(24) Xu, W.; Sun, Y.; Wang, Q.; Du, W.; Zhao, J.; Ge, X.; Han, T.; Zhang, Y.; Zhou, W.; Li, J.; Fu, P.; Wang, Z.; Worsnop, D. R. Seasonal Characterization of Organic Nitrogen in Atmospheric Aerosols Using High Resolution Aerosol Mass Spectrometry in Beijing, China. *ACS Earth Space Chem.* **2017**, *1*, 673−682.

(25) Sharma, E. Reconciling Mountain Biodiversity Conservation and Human Wellbeing: Drivers of Biodiversity Loss and New Approaches in the Hindu-Kush Himalayas. *Proc. Indian Natl. Sci. Acad.* **2016**, *82*, 53−73.

(26) Kang, S.; Mayewski, P. A.; Qin, D.; Yan, Y.; Zhang, D.; Hou, S.; Ren, J. Twentieth century increase of atmospheric ammonia recorded in Mount Everest ice core. *J. Geophys. Res.: Atmos.* **2002**, *107*, ACL 13-1−ACL 13-9.

(27) Zheng, W.; Yao, T.; Joswiak, D. R.; Xu, B.; Wang, N.; Zhao, H. Major ions composition records from a shallow ice core on Mt. Tanggula in the central Qinghai-Tibetan Plateau. *Atmos. Res.* **2010**, *97*, 70−79.

(28) Zhao, Y.; Zhang, L.; Chen, Y.; Liu, X.; Xu, W.; Pan, Y.; Duan, L. Atmospheric nitrogen deposition to China: A model analysis on nitrogen budget and critical load exceedance. *Atmos. Environ.* **2017**, *153*, 32−40.

(29) Liu, B.; Kang, S.; Sun, J.; Zhang, Y.; Xu, R.; Wang, Y.; Liu, Y.; Cong, Z. Wet precipitation chemistry at a high-altitude site (3,326 m a.s.l.) in the southeastern Tibetan Plateau. *Environ. Sci. Pollut. Res.* **2013**, *20*, 5013−5027.

(30) Bobbink, R.; Hicks, K.; Galloway, J.; Spranger, T.; Alkemade, R.; Ashmore, M.; Bustamante, M.; Cinderby, S.; Davidson, E.; Dentener, F.; Emmett, B.; Erisman, J.-W.; Fenn, N.; Gilliam, F.; Nordin, A.; Pardo, L.; de Vries, W. Global assessment of nitrogen deposition effects on terrestrial plant diversity: a synthesis. *Ecol. Appl.* **2010**, *20*, 30−59.

(31) Zhao, Z.; Cao, J.; Shen, Z.; Xu, B.; Zhu, C.; Chen, L. W. A.; Su, X.; Liu, S.; Han, Y.; Wang, G.; Ho, K. Aerosol particles at a high-altitude site on the Southeast Tibetan Plateau, China: Implications for pollution transport from South Asia. *J. Geophys. Res.: Atmos.* **2013**, *118*, 11,360−11,375.

(32) Wu, G.; Wan, X.; Gao, S.; Fu, P.; Yin, Y.; Li, G.; Zhang, G.; Kang, S.; Ram, K.; Cong, Z. Humic-like substances (HULIS) in aerosols of central Tibetan Plateau (Nam Co, 4730 m asl): Abundance, light absorption properties and sources. *Environ. Sci. Technol.* **2018**, *52*, 7203−7211.

(33) Fan, M.-Y.; Zhang, Y.-L.; Lin, Y.-C.; Chang, Y.-H.; Cao, F.; Zhang, W.-Q.; Hu, Y.-B.; Bao, M.-Y.; Liu, X.-Y.; Zhai, X.-Y.; Lin, X.; Zhao, Z.-Y.; Song, W.-H. Isotope-based source apportionment of nitrogen-containing aerosols: A case study in an industrial city in China. *Atmos. Environ.* **2019**, *212*, 96−105.

(34) Draxler, R.; Rolph, G. *HYSPLIT (HYbrid Single-Particle Lagrangian Integrated Trajectory) Model*; NOAA Air Resources Laboratory: Silver Spring, MD. *Access via NOAA ARL READY Website* 2003.

(35) Naja, M.; Akimoto, H.; Staehelin, J. Ozone in background and photochemically aged air over central Europe: Analysis of long-term ozonesonde data from Hohenpeissenberg and Payerne. *J. Geophys. Res.: Atmos.* **2003**, *108*, 4063.

(36) Stohl, A. Evaluation of trajectories calculated from ECMWF data against constant volume balloon flights during ETEX. *Atmos. Environ.* **1998**, *32*, 4151−4156.

(37) Duce, R. A.; Liss, P. S.; Merrill, J. T.; Atlas, E. L.; Buat-Menard, P.; Hicks, B. B.; Miller, J. M.; Prospero, J. M.; Arimoto, R.; Church, T. M.; Ellis, W.; Galloway, J. N.; Hansen, L.; Jickells, T. D.; Knap, A. H.; Reinhardt, K. H.; Schneider, B.; Soudine, A.; Tokos, J. J.; Tsunogai, S.; Wollast, R.; Zhou, M. The atmospheric input of trace species to the world ocean. *Global Biogeochem. Cycles* **1991**, *5*, 193−259.

(38) He, J.; Balasubramanian, R.; Burger, D. F.; Hicks, K.; Kuylenstierna, J. C.; Palani, S. Dry and wet atmospheric deposition of nitrogen and phosphorus in Singapore. *Atmos. Environ.* **2011**, *45*, 2760−2768.

(39) Fu, Y.; Wang, W.; Han, M.; kuerban, M.; Wang, C.; Liu, X. Atmospheric dry and bulk nitrogen deposition to forest environment in the North China Plain. *Atmos. Pollut. Res.* **2019**, *10*, 1636−1642.

(40) Chen, H.-Y.; Huang, S.-Z. Effects of Atmospheric Dry Deposition on External Nitrogen Supply and New Production in the Northern South China Sea. *Atmosphere* **2018**, *9*, 386.

(41) Kunwar, B.; Kawamura, K.; Zhu, C. Stable carbon and nitrogen isotopic compositions of ambient aerosols collected from Okinawa Island in the western North Pacific Rim, an outflow region of Asian dusts and pollutants. *Atmos. Environ.* **2016**, *131*, 243−253.

(42) Xiao, H.-W.; Xiao, H.-Y.; Luo, L.; Zhang, Z.-Y.; Huang, Q.-W.; Sun, Q.-B.; Zeng, Z.-q. Stable carbon and nitrogen isotope compositions of bulk aerosol samples over the South China Sea. *Atmos. Environ.* **2018**, *193*, 1−10.

(43) Mkoma, S. L.; Kawamura, K.; Tachibana, E.; Fu, P. Stable carbon and nitrogen isotopic compositions of tropical atmospheric aerosols: sources and contribution from burning of C_3 and C_4 plants to organic aerosols. *Tellus B* **2014**, *66*, 20176.

(44) Uematsu, M.; Kawamura, K.; Ibusuki, T.; Kimoto, T. Chemical composition of marine aerosols over the Central North Pacific—Results from the 1991 cruise of Hakurei Maru No. 2—. In *Biogeochemical Processes and Ocean Flux in the Western Pacific*; Terra Scientific Publishing Company: 1995, 3−14.

(45) Lin, M.; Walker, J.; Geron, C.; Khlystov, A. Organic nitrogen in $PM_{2.5}$ aerosol at a forest site in the Southeast US. *Atmos. Chem. Phys.* **2010**, *10*, 2145−2157.

(46) Chelani, A. B.; Gajghate, D. G.; ChalapatiRao, C. V.; Devotta, S. Particle size distribution in ambient air of Delhi and its statistical analysis. *Bull. Environ. Contam. Toxicol.* **2010**, *85*, 22−27.

(47) Kawamura, K.; Kobayashi, M.; Tsubonuma, N.; Mochida, M.; Watanabe, T.; Lee, M. Organic and inorganic compositions of marine aerosols from East Asia: Seasonal variations of water-soluble dicarboxylic acids, major ions, total carbon and nitrogen, and stable C and N isotopic composition. *Geochem. Soc. Spec. Publ.* **2004**, *9*, 243−265.

(48) Pavuluri, C. M.; Kawamura, K.; Tachibana, E.; Swaminathan, T. Elevated nitrogen isotope ratios of tropical Indian aerosols from Chennai: implication for the origins of aerosol nitrogen in South and Southeast Asia. *Atmos. Environ.* **2010**, *44*, 3597−3604.

(49) Agnihotri, R.; Mandal, T. K.; Karapurkar, S. G.; Naja, M.; Gadi, R.; Ahammmed, Y. N.; Kumar, A.; Saud, T.; Saxena, M. Stable carbon and nitrogen isotopic composition of bulk aerosols over India and northern Indian Ocean. *Atmos. Environ.* **2011**, *45*, 2828−2835.

(50) Turekian, V. C.; Macko, S.; Ballentine, D.; Swap, R. J.; Garstang, M. Causes of bulk carbon and nitrogen isotopic fractionations in the products of vegetation burns: laboratory studies. *Chem. Geol.* **1998**, *152*, 181−192.

(51) Kundu, S.; Kawamura, K.; Andreae, T. W.; Hoffer, A.; Andreae, M. O. Diurnal variation in the water-soluble inorganic ions, organic carbon and isotopic compositions of total carbon and nitrogen in biomass burning aerosols from the LBA-SMOCC campaign in Rondônia, Brazil. *J. Aerosol Sci.* **2010**, *41*, 118−133.

DOI: 10.1021/acs.est.9b03999
Environ. Sci. Technol. XXXX, XXX, XXX−XXX

(52) Agnihotri, R.; Karapurkar, S. G.; Sarma, V. V. S. S.; Yadav, K.; Kumar, M. D.; Sharma, C.; Prasad, M. V. S. N. Stable isotopic and chemical characteristics of bulk aerosols during winter and summer Seasons at a station in western coast of India (Goa). *Aerosol Air Qual. Res.* **2015**, *15*, 888−900.
(53) Martinelli, L.; Camargo, P.; Lara, L.; Victoria, R.; Artaxo, P. Stable carbon and nitrogen isotopic composition of bulk aerosol particles in a C4 plant landscape of southeast Brazil. *Atmos. Environ.* **2002**, *36*, 2427−2432.
(54) Morera-Gomez, Y.; Santamaria, J. M.; Elustondo, D.; Alonso-Hernandez, C. M.; Widory, D. Carbon and nitrogen isotopes unravels sources of aerosol contamination at Caribbean rural and urban coastal sites. *Sci. Total Environ.* **2018**, *642*, 723−732.
(55) Shakya, K. M.; Ziemba, L. D.; Griffin, R. J. Characteristics and sources of carbonaceous, ionic, and isotopic species of wintertime atmospheric aerosols in Kathmandu Valley, Nepal. *Aerosol Air Qual. Res* **2010**, *10*, 219−230.
(56) Aggarwal, S. G.; Kawamura, K.; Umarji, G. S.; Tachibana, E.; Patil, R. S.; Gupta, P. K. Organic and inorganic markers and stable C-, N-isotopic compositions of tropical coastal aerosols from megacity Mumbai: sources of organic aerosols and atmospheric processing. *Atmos. Chem. Phys.* **2013**, *13*, 4667−4680.
(57) Boreddy, S. K. R.; Parvin, F.; Kawamura, K.; Zhu, C.; Lee, C.-T. Stable carbon and nitrogen isotopic compositions of fine aerosols ($PM_{2.5}$) during an intensive biomass burning over Southeast Asia: Influence of SOA and aging. *Atmos. Environ.* **2018**, *191*, 478−489.
(58) Bhattarai, H.; Saikawa, E.; Wan, X.; Zhu, H.; Ram, K.; Gao, S.; Kang, S.; Zhang, Q.; Zhang, Y.; Wu, G.; Wang, X.; Kawamura, K.; Fu, P.; Cong, Z. Levoglucosan as a tracer of biomass burning: Recent progress and perspectives. *Atmos. Res.* **2019**, *220*, 20−33.
(59) Urban, R. C.; Lima-Souza, M.; Caetano-Silva, L.; Queiroz, M. E. C.; Nogueira, R. F. P.; Allen, A. G.; Cardoso, A. A.; Held, G.; Campos, M. L. A. M. Use of levoglucosan, potassium, and water-soluble organic carbon to characterize the origins of biomass-burning aerosols. *Atmos. Environ.* **2012**, *61*, 562−569.
(60) Andreae, M. O.; Browell, E. V.; Garstang, M.; Gregory, G. L.; Harriss, R. C.; Hill, G. F.; Jacob, D. J.; Pereira, M. C.; Sachse, G. W.; Setzer, A. W.; Dias, P. L. S.; Talbot, R. W.; Torres, A. L.; Wofsy, S. C. Biomass-burning emissions and associated haze layers over Amazonia. *J. Geophys. Res.: Atmos.* **1988**, *93*, 1509−1527.
(61) Engling, G.; Zhang, Y.-N.; Chan, C.-Y.; Sang, X.-F.; Lin, M.; Ho, K.-F.; Li, Y.-S.; Lin, C.-Y.; Lee, J. J. Characterization and sources of aerosol particles over the southeastern Tibetan Plateau during the Southeast Asia biomass-burning season. *Tellus B* **2011**, *63*, 117−128.
(62) Cong, Z.; Kang, S.; Kawamura, K.; Liu, B.; Wan, X.; Wang, Z.; Gao, S.; Fu, P. Carbonaceous aerosols on the south edge of the Tibetan Plateau: concentrations, seasonality and sources. *Atmos. Chem. Phys.* **2015**, *15*, 1573−1584.
(63) Li, J.; Pósfai, M.; Hobbs, P. V.; Buseck, P. R. Individual aerosol particles from biomass burning in southern Africa: 2, Compositions and aging of inorganic particles. *J. Geophys. Res.: Atmos.* **2003**, *108*, 8484.
(64) Singh, N.; Banerjee, T.; Raju, M. P.; Deboudt, K.; Sorek-Hamer, M.; Singh, R. S.; Mall, R. K. Aerosol chemistry, transport, and climatic implications during extreme biomass burning emissions over the Indo-Gangetic Plain. *Atmos. Chem. Phys.* **2018**, *18*, 14197−14215.
(65) Ram, K.; Sarin, M. M.; Sudheer, A. K.; Rengarajan, R. Carbonaceous and Secondary Inorganic Aerosols during Wintertime Fog and Haze over Urban Sites in the Indo-Gangetic Plain. *Aerosol Air Qual. Res.* **2012**, *12*, 359−370.
(66) Sawlani, R.; Agnihotri, R.; Sharma, C.; Patra, P. K.; Dimri, A. P.; Ram, K.; Verma, R. L. The severe Delhi SMOG of 2016: A case of delayed crop residue burning, coincident firecracker emissions, and atypical meteorology. *Atmos. Pollut. Res.* **2019**, *10*, 868−879.
(67) Cong, Z.; Kawamura, K.; Kang, S.; Fu, P. Penetration of biomass-burning emissions from South Asia through the Himalayas: new insights from atmospheric organic acids. *Sci. Rep.* **2015**, *5*, 9580.
(68) Liu, X.; Duan, L.; Mo, J.; Du, E.; Shen, J.; Lu, X.; Zhang, Y.; Zhou, X.; He, C.; Zhang, F. Nitrogen deposition and its ecological impact in China: an overview. *Environ. Pollut.* **2011**, *159*, 2251−2264.
(69) Vitousek, P. M.; Aber, J. D.; Howarth, R. W.; Likens, G. E.; Matson, P. A.; Schindler, D. W.; Schlesinger, W. H.; Tilman, D. G. Human alteration of the global nitrogen cycle: sources and consequences. *Ecol. Appl.* **1997**, *7*, 737−750.
(70) Burns, D. A. Atmospheric nitrogen deposition in the Rocky Mountains of Colorado and southern Wyoming—a review and new analysis of past study results. *Atmos. Environ.* **2003**, *37*, 921−932.
(71) Xu, W.; Luo, X. S.; Pan, Y. P.; Zhang, L.; Tang, A. H.; Shen, J. L.; Zhang, Y.; Li, K. H.; Wu, Q. H.; Yang, D. W.; et al. Quantifying atmospheric nitrogen deposition through a nationwide monitoring network across China. *Atmos. Chem. Phys.* **2015**, *15*, 12345−12360.

DOI: 10.1021/acs.est.9b03999
Environ. Sci. Technol. XXXX, XXX, XXX−XXX